

# Oxygen and acrylamide quenching of protein phosphorescence: correlation with protein dynamics

Patrizia Cioni\*

*Istituto di Biofisica, Consiglio Nazionale delle Ricerche, Area della Ricerca di Pisa, Via Alfieri 1, San Cataldo,  
56010 Ghezzano, Pisa, Italy*

Received 7 March 2000; received in revised form 31 May 2000; accepted 1 June 2000

## Abstract

Oxygen quenching of protein phosphorescence and activation enthalpies for the structural fluctuations underlying  $O_2$  and acrylamide diffusion were determined for RNase T1, glyceraldehyde-3-phosphate dehydrogenase and  $\beta$ -lactoglobulin, which have the phosphorescing residues located in relatively solvent-exposed and flexible regions of the polypeptide. The results, compared with those obtained for proteins characterised by a very rigid environment, established that  $kq_{O_2}$  was directly correlated to the flexibility of the protein matrix surrounding the chromophore. While the migration of acrylamide was characterised by  $\Delta H^\ddagger$ , which was strongly dependent on the fluidity of the structure about the Trp residue, the values of the activation enthalpies for the oxygen migration of all the proteins studied were rather similar,  $\sim 10 \text{ kcal mol}^{-1}$ , in spite of the depth of the chromophore and the rigidity of its environment. The implications of these findings for the migration of small solutes inside proteins have been discussed. © 2000 Elsevier Science B.V. All rights reserved.

**Keywords:** Phosphorescence; Tryptophan; Oxygen; Acrylamide; Quenching; Protein dynamics

**Abbreviations:** Az, apoazurin; LADH, horse liver alcohol dehydrogenase; AP, alkaline phosphatase; NATA, N-acetyl-tryptophanamide; kq, bimolecular quenching constant; GAPDH, glyceraldehyde-3-phosphate dehydrogenase; RNase T1, ribonuclease T1;  $\beta$ -LG,  $\beta$ -lactoglobulin; W, tryptophan;  $\tau_0$ , phosphorescence lifetime

\*Tel.: +39-050315-3051; fax: +39-050315-2760.

E-mail address: patrizia@ib.pi.cnr.it (P. Cioni).

## 1. Introduction

X-Ray crystallographic and NMR studies have provided a library of detailed protein structure. However, the structures by themselves supply a description of a static or dynamically averaged picture of the molecule, while the macromolecular function is, in many cases, coupled to flexibility. Several experimental approaches have demonstrated conformational dynamics within the protein structure, and their ultimate goal was to illustrate how motion relates to function and stability [1,2]. Much can be learned about the frequency and the amplitude of structural fluctuations in globular proteins by monitoring the diffusion of solutes of variable sizes through a generally compact globular fold. One method to measure the permeability of the protein matrix to small molecules was based on the rate by which the fluorescence or phosphorescence emission of internal Trp residues is quenched by solutes that come into their proximity [3–5]. Quenching experiments determine the excited state lifetime ( $\tau$ ) as a function of the quencher concentration in solution,  $[Q]$ , and evaluate the bimolecular quenching constant,  $kq$ , from the gradient of the Stern–Volmer plot:  $1/\tau = 1/\tau_0 + kq[Q]$ , where  $\tau_0$  is the unperturbed lifetime. For reactions that are under diffusion control,  $kq \propto D$ , where  $D$  is essentially the diffusion coefficient of  $Q$  inside the protein matrix. Initial studies by Lakowicz and Weber on the oxygen quenching of protein fluorescence [6] led to the conclusion that fluctuations of the polypeptide occur in a nanosecond time-scale to allow the free diffusion of  $O_2$  through any protein matrix. Recently, however, studies on oxygen and acrylamide quenching of Trp phosphorescence in proteins [7,8] have shown that, even in the long millisecond–second time scale of the delayed emission, globular proteins may oppose a considerable barrier to the reaction between these quenchers and the triplet state of tryptophan; the quenching rate constants decreasing monotonically with both the degree of burial of the chromophore and the rigidity of the embedding protein structure, the latter monitored by the empirical relationship between the triplet lifetime ( $\tau_0$ ) and the medium viscosity [9]. Accord-

ing to these findings, the rate of  $O_2$  migration reflects the flexibility of the globular fold and, therefore, represents a monitor of protein conformational dynamics, even if it is far less sensitive in comparison to acrylamide, as oxygen diffuses more readily through the macromolecule. These conclusions are based only on three proteins (apoazurin, alkaline phosphatase and alcohol dehydrogenase) and these are characterised by a very rigid environment about the triplet probe.

The aim of the present investigation was to verify the generality of these conclusions by extending the study to proteins with phosphorescent tryptophan residues located in more solvent-exposed and flexible regions of the polypeptide. Structural fluctuations in these proteins are also characterised by the temperature dependence of  $kq$  for both  $O_2$  and acrylamide, as well as  $\tau_0$ . The three systems chosen were structurally and spectroscopically well-characterised proteins: RNase T1, yeast glyceraldehyde 3-phosphate dehydrogenase, and bovine  $\beta$ -lactoglobulin. The high resolution X-ray structure of RNase T1 from *Aspergillus oryzae* shows that the indole side chain of its sole Trp (W59) is wrapped within the central  $\beta$ -sheet. Although it is tucked away from the solvent interface, 2 Å from the aqueous surface, a five-water molecule chain connects the indole ring to bulk solvent, thereby making the site rather flexible. Consistent with a mobile environment, the lifetime of Trp59 is relatively small (31 ms) [10]. Tetrameric GAPDH exhibits an intense and long-lived room temperature phosphorescence from a single Trp residue in each subunit, and its location is relatively well-known. In fact, although there were three Trp residues present in each subunit (W84, W193, W310), by analogy with GAPDH from *B. stearothermophilus*, the phosphorescing residue was likely to be Trp 84 which was 5.5 Å from the aqueous interface [11]. Bovine  $\beta$ -LG is a small globular protein with eight strands of antiparallel  $\beta$ -sheets twisted into a cone-shaped barrel, which constitutes a hydrophobic pocket.  $\beta$ -LG has two tryptophanyl residues per subunit. Trp-19 is at the bottom of the central hydrophobic calix of the protein, 6 Å from the surface, while Trp-61 is part of an external loop. It was proposed that the fluorescence of Trp-61 is

quenched in the native protein, possibly by the nearby cystine 160–166 disulfide bond [12]. For this reason and because of the external location of the Trp 61, the phosphorescence emission was attributed exclusively to Trp 19 [13]. The triplet lifetime at 20°C of RNase T1,  $\beta$ -LG and GAPDH was 31, 50 and 200 ms, respectively. From the empirical correlation between  $\tau_0$  and local viscosity [9], it could be deduced that, although the polypeptide about the three phosphorescing residues was relatively well structured, it was less rigid than the examples studied previously.

The findings reported in this study confirmed that, even for these relatively flexible sites,  $O_2$  diffusion was slowed down relative to diffusion in water, and that the quenching rate constants were directly correlated to the viscosity of the protein matrix surrounding the chromophore, as deduced from  $\tau_0$  and the acrylamide quenching rate constants. From the temperature dependence of  $kq$  it was concluded that the activation barrier to  $O_2$  migration was surprisingly similar to that reported for more internal and rigid protein sites; a behaviour which was in contrast with what it was observed for acrylamide migration and the relaxation of the excited triplet state.

## 2. Materials and methods

Ribonuclease  $T_1$  was purchased from Calbiochem Corporation (San Diego, CA). The proteins: horse liver alcohol dehydrogenase, and glyceraldehyde-3-phosphate dehydrogenase from yeast, were supplied by Boehringer (Mannheim, Germany). To remove  $NAD^+$  from GAPDH, the enzyme was treated with activated charcoal, as previously reported by Strambini and Gabellieri [14].  $\beta$ -lactoglobulin A was obtained from Sigma. Water, doubly distilled over quartz, was purified by a Milli-Q Plus system (Millipore Corporation, Bedford, MA). All glassware used for sample preparation was conditioned in advance by standing for 24 h in 10% HCl suprapur (Merck, Darmstadt).

### 2.1. Luminescence measurements

Fluorescence and phosphorescence spectra, in-

tensities and phosphorescence decay kinetics were obtained with a home-made apparatus, as previously described by Gonnelli and Strambini [15,16]. Briefly, continuous excitation for fluorescence and phosphorescence spectra was provided by a Cermax xenon lamp (LX 150 UV, ILC) and the excitation wavelength, typically 290 nm, was selected by a 0.25-m grating monochromator (model 82-410, Jarrel-Ash) with a 10-nm bandpass. The emission collected through another 0.25-m grating monochromator (Jobin-Yvon, H25) with a 7-nm bandwidth was detected by an EMI9635QB photomultiplier. Phosphorescence decays were obtained with pulsed excitation as provided by a frequency-doubled flash-pumped dye laser (UV500M Candela) tuned at 292 nm. The pulse duration was 1  $\mu$ s and the light energy per pulse was, typically, 1–10 mJ. The phosphorescence signal collected at a right angle from the excitation beam was filtered (420–460-nm band pass) and detected by an R928 photomultiplier. An electronic shutter arrangement protected the photomultiplier from the intense fluorescence pulse and permitted the delayed emission to be detected 4 ms after the excitation pulse. Alternatively, for lifetimes shorter than 5 ms, the photomultiplier was protected from the intense fluorescence pulse by a chopper blade that closes the emission slit during the excitation. The time resolution of this apparatus was, typically, 10  $\mu$ s [15]. The photocurrent was amplified by a current-to-voltage converter (SR570, Stanford Research Systems), and digitised by a computerscope system (ISC-16, RC Electronics) capable of averaging multiple sweeps. All phosphorescence decays were analysed in terms of the sum of exponential components by a non-linear least-squares fitting algorithm (Global Unlimited, LFD, University of Illinois). The lifetime data used in the analysis were averages of two or more independent measurements. The reproducibility of phosphorescence lifetimes was typically better than 5%.

### 2.2. Sample preparation for phosphorescence measurements

Prior to phosphorescence measurements, all proteins were extensively dialysed in Tris-HCl (10

mM, pH 7.5). For measurements of the intrinsic phosphorescence lifetime, it was paramount to rid the solution of all  $O_2$  traces. The deoxygenation of the protein samples was carried out by repeated cycles of mild evacuation, followed by the inlet of pure nitrogen as described by Strambini [16]. Determinations of the  $O_2$ -quenching rate constants were made, utilising the phosphorescence of a protein of known  $kq_{O_2}$  as an internal monitor of  $[O_2]$  in solution, as described by Strambini and Cioni [8]. For this study, the internal reference protein was LADH, instead of alkaline phosphatase, because its  $kq_{O_2}$  was closer to that of the proteins under investigation. In  $O_2$ -quenching experiments with samples of RNase T1,  $\beta$ -LG and GAPDH, containing approximately 20% LADH (on a chromophore basis), various  $O_2$  contents were simply attained by interrupting the initial de-oxygenation of the solution at various stages before completion. The bimolecular quenching rate constant ( $k_q$ ) was obtained from measurements of the phosphorescence decay at various  $[O_2]$ , according to the equation:

$$1/\tau = (1/\tau_0) + kq[O_2] \quad (1)$$

where  $\tau_0$  and  $\tau$  are the phosphorescence lifetime in the absence and in the presence of a given  $[O_2]$ , respectively.  $[O_2]$  was determined from its effect on the phosphorescence lifetime of LADH in the same solution. At least five different  $[O_2]$  were employed in the construction of the Stern–Volmer plots.

### 3. Results and discussion

#### 3.1. $O_2$ quenching of RNase T1, $\beta$ -LG and GAPDH phosphorescence

In the presence of  $O_2$ , the phosphorescence of RNase T1,  $\beta$ -LG and GAPDH was shorter lived and its decay was strictly exponential, even if the emission of the last two proteins in the absence of oxygen was heterogeneous. An example of the phosphorescence decay of RNase T1, at 20°C, in

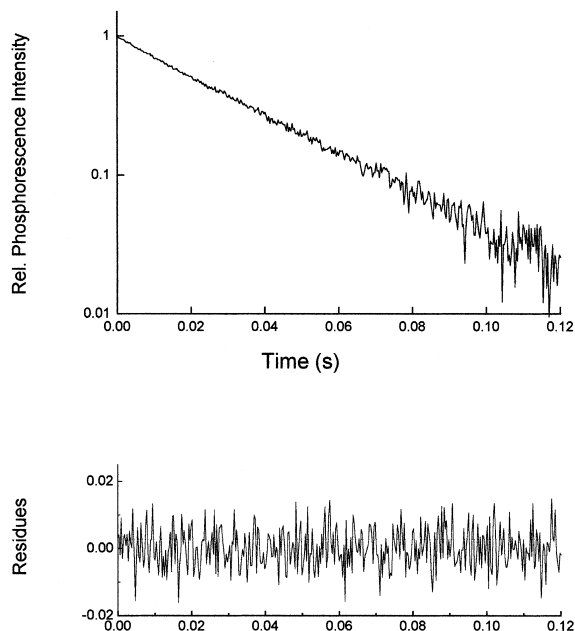


Fig. 1. Example of primary phosphorescence decay data and fitting statistics. The sample is 2  $\mu$ M RNase T1 in Tris-HCl (10 mM, pH 7.5) at 20°C. The decay signal is from a single sweep. In the bottom panel, the residues of a single exponential analysis are displayed.

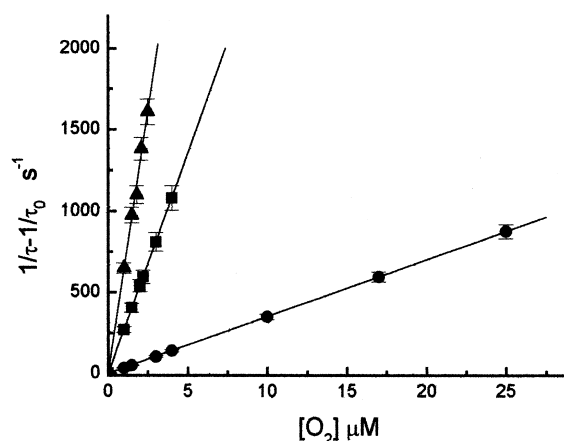


Fig. 2. Lifetime Stern–Volmer plots for the quenching of protein phosphorescence by  $O_2$ . The protein samples are in 10 mM Tris-HCl buffer, pH 7.5, at 20°C. The variation of the slope among independent sets of experiments is less than 10%. The proteins samples are:  $\beta$ -LG (■), GAPDH (●) and RNase T1 (▲).

Table 1  
Acrylamide and oxygen bimolecular phosphorescence quenching rate constant for NATA and for internal Trp residues in proteins, at 20°C<sup>a</sup>

| Protein A | Trp # | $r_p$ (Å) | $\tau_0$ (ms) <sup>c</sup> | $kq$ (O <sub>2</sub> ) <sup>d</sup><br>(M <sup>-1</sup> s <sup>-1</sup> ) | $kq$ (acr) <sup>d</sup><br>(M <sup>-1</sup> s <sup>-1</sup> ) | $\eta$ (O <sub>2</sub> ) <sup>b</sup><br>(cP) | $\eta$ (acr) <sup>b</sup><br>(cP) | $\eta$ ( $\tau_0$ ) <sup>b</sup><br>(cP) |
|-----------|-------|-----------|----------------------------|---|---|---|-----------------------------------|--|
| NATA      |       |           |                            | $5.0 \times 10^9$   | $1.5 \times 10^9$   |   |                                   |  |
| LADH      | 314   | 4.5       | 628                        | $2.8 \times 10^7$   | $1.2 \times 10^4$   | $2.0 \times 10^2$                             | $1.2 \times 10^5$                 | $4.9 \times 10^4$                        |
| Az        | 48    | 8         | 600                        | $7.5 \times 10^6$   | 32  | $6.7 \times 10^2$                             | $4.6 \times 10^7$                 | $4.6 \times 10^4$                        |
| AP        | 109   | 11        | 2060                       | $1.2 \times 10^6$   | 0.1   | $4.2 \times 10^3$                             | $1.5 \times 10^{10}$              | $7.5 \times 10^4$                        |
| Rnase T1  | 59    | 2         | 31                         | $6.5 \times 10^8$   | $5.9 \times 10^4$   | 8   | $2.5 \times 10^4$                 | $5.0 \times 10^2$                        |
| β-LG      | 19    | 6         | 50                         | $2.7 \times 10^8$   | $4.2 \times 10^4$   | 18  | $3.6 \times 10^4$                 | $7.1 \times 10^2$                        |
| GAPDH     | 84    | 5.5       | 200                        | $3.5 \times 10^7$   | $3.4 \times 10^2$   | 140   | $4.4 \times 10^6$                 | $5.4 \times 10^3$                        |

<sup>a</sup>Triplet lifetime, crystallographic data ( $r_p$ ) and comparison of the internal protein viscosity monitored by the same Trp probe according to  $kq$  (O<sub>2</sub>),  $kq$  (acr) and  $\tau_0$  are also included.

<sup>b</sup>Data at 20°C.  $\eta_{\text{prot}}$  is obtained from either  $kq(\text{solv})/kq(\text{prot})$  or from the empirical relationship between  $\tau_0$  and solvent viscosity in model studies [9].

<sup>c</sup>The reproducibility of lifetime measurements is typically 5% or better.

<sup>d</sup>The S.E. is less than 9%.

the absence of oxygen, is shown in Fig. 1. The Stern–Volmer plots at 20°C are shown in Fig. 2 and the bimolecular quenching rate constants,  $k_{qO_2}$ , derived from their slopes are given in Table 1. Relative to the quenching of free tryptophan ( $k_{qO_2} = 5 \times 10^9 \text{ M}^{-1} \text{ s}^{-1}$ ) [17], the rate for the buried residues of RNase T1,  $\beta$ -LG and GAPDH was  $6.5 \times 10^8$ ,  $2.7 \times 10^8$  and  $3.5 \times 10^7 \text{ M}^{-1} \text{ s}^{-1}$ , respectively, 1–2 orders of magnitude smaller, and this implied that  $O_2$  diffusion into these internal protein sites was slowed down relative to diffusion in water by at least the same factor. Compared to the phosphorescence quenching constants of the proteins studied previously (LADH, Az, AP) [8], also reported in Table 1, the magnitude of  $k_{qO_2}$  for RNase T1 and  $\beta$ -LG was distinctly larger, whereas for GAPDH it was similar to LADH. Overall, the widest range of  $k_{qO_2}$  was between AP and RNase T1, which varied by a factor of  $\sim 10^3$ .

It is interesting to investigate the molecular factors that could be responsible for these differences. One parameter could be the proximity of the triplet probe to the solvent. Although the results of the present study confirmed that, for buried Trp residues  $k_{qO_2}$  could be much smaller than for residues that were on the protein surface, no simple relationship was found between the value of  $k_{qO_2}$  and the closest distance of the triplet probe from the surface ( $r_p$ ). For instance, GAPDH and  $\beta$ -LG had practically the same  $r_p$ , but very different  $k_{qO_2}$ . For RNase T1, the analysis of  $k_{qO_2}$  in terms of  $r_p$  could also be complicated by through-space quenching by  $O_2$  in the solvent, because the 2-Å separation of the chromophore (W59) from the aqueous interface [10] could make this process competitive with diffusive pathways. This ambiguity on the quenching mechanism should not apply to the other two proteins that had an  $r_p$  value larger than 5 Å. This is because, for LADH ( $r_p = 4.5 \text{ Å}$ ), it was shown that through-space interactions did not seem to compete with quenching by  $O_2$  migration [8]. Another parameter that should be directly correlated with the rate of oxygen migration is the flexibility of the protein matrix. It is interesting to compare the oxygen quenching rate constants with the estimate of the local viscosity made by the

same probe (Trp residue) based on different phenomena. Direct monitors of the protein ‘microviscosity’ in the region surrounding the chromophore were provided by the intrinsic phosphorescence lifetime,  $\tau_0$ , ( $\eta_{\tau_0}$ ) [9] and by the reduction of the acrylamide phosphorescence quenching rate constant ( $k_{q_{acr}}$ ), relative to that of the chromophore in solution [5,7].

As shown in Table 1, the apparent frictional drag governing  $O_2$  diffusion in RNase T1,  $\beta$ -LG and GAPDH, was invariably much lower than that anticipated on the basis of the local viscosity estimated by  $\tau_0$  ( $\eta_{\tau_0}$ ), and even more so on the basis of acrylamide quenching ( $k_{q_{acr}}$ ). This suggested that not all the structural fluctuations that permit  $O_2$  migration were efficacious in deactivating the triplet state, and even fewer were those that allow acrylamide diffusion. Clearly the different appraisals of the internal protein viscosity by the two quenchers was imputable to their different sizes, in that only large amplitude fluctuations permitted the migration of the bulkier acrylamide. Fig. 3 shows the protein viscosities, as inferred from the migration of  $O_2$  and of acrylamide vs. the viscosity obtained by  $\tau_0$ . Except for LADH, the plots indicated a clear correlation between these parameters: the tighter the protein matrix around the chromophore, inferred from  $\tau_0$ , the more hindered the migration of the two quenchers. A possible explanation for the exception of LADH is that its triplet probe, W314, lies at the subunit interface of the dimeric molecule and quencher permeation may have been facilitated by transient partial subunit dissociation. In consideration of the complete disregard for individual details of secondary and tertiary structure, and of the many possibilities for a discordant estimate of the ‘internal viscosity’ by  $\tau_0$  and  $kq$ , such a correlation between totally independent parameters was significant. It should be noted that, because  $\tau_0$  was a probe of the local flexibility of the structure around the tryptophan, whereas the migration of oxygen and acrylamide could be limited by barriers beyond this core, a strict correlation between quenching rate constants and  $\tau_0$  was not expected. The relationship found between these parameters suggested that the rate-limiting step for the quenching reaction was due to the

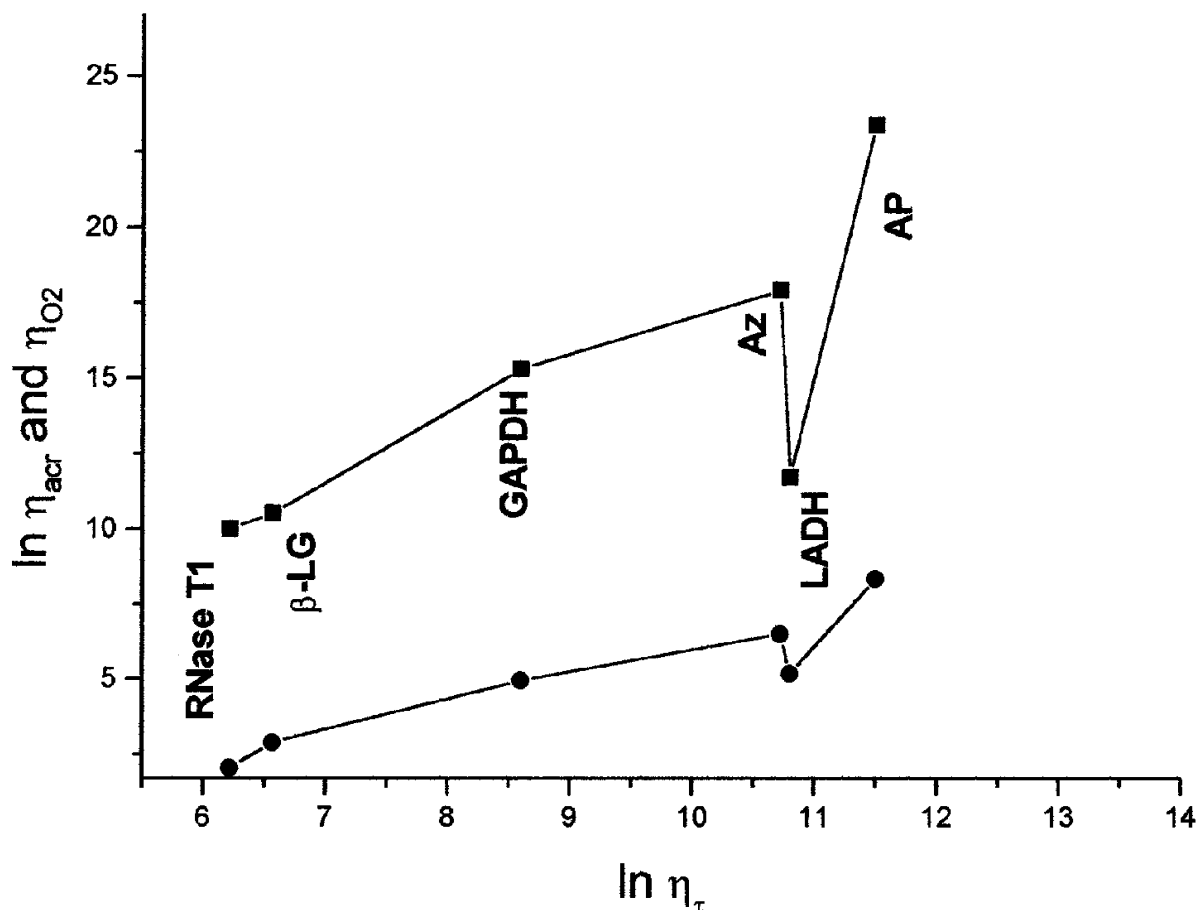


Fig. 3. Logarithmic plot of the viscosity inferred at 20°C from the quenching rate constant of acrylamide ( $\eta_{acr}$ ) (■) and  $O_2$  ( $\eta_{O_2}$ ) (●) vs. the viscosity derived from  $\tau_0$  for the proteins of Table 1.

migration of the molecules through the rigid cores around the triplet probe, and that even for the relatively mobile regions of  $\beta$ -LG and GAPDH,  $O_2$  diffusion was governed by conformational dynamics.

All comparisons between studies of fluorescence and phosphorescence quenching rate constants obtained for the same Trp residues have yielded discrepant estimates of the oxygen diffusion in proteins [3,4,16]. Possible explanations of this disagreement have been discussed by Strambini and Cioni in a previous paper [8]. Among the three proteins analysed in this report, it was possible to make such a comparison only for RNase T1. The difference in the values of the two

quenching rate constants ( $2.3 \times 10^9 \text{ M}^{-1} \text{ s}^{-1}$  for fluorescence [4] and  $6.5 \times 10^8 \text{ M}^{-1} \text{ s}^{-1}$  for phosphorescence) was what we would expect considering the spin factor (from 1/5 to 1/9). It should be recalled that the largest difference between the fluorescence and phosphorescence quenching rate constants (as much as a factor of  $10^3$  for W109 of AP) was observed for residues deeply buried in the rigid cores of the globular structure. The good agreement found for solvent-exposed W59 of RNase T1 ( $r_p = 2 \text{ \AA}$ ) drew our attention to the fact that the discrepancy between the rates decreased the closer the chromophore was located to the protein surface. A possible explanation for this behaviour is that over distance of a

Table 2

Activation enthalpies obtained from the temperature dependence of  $\eta(\tau_0)$  and of acrylamide and oxygen bimolecular phosphorescence quenching rate constant

| Protein A   | $\Delta H^\ddagger (kq_{O_2})$<br>(kcal mol <sup>-1</sup> ) | $\Delta H^\ddagger (kq_{acr})$<br>(kcal mol <sup>-1</sup> ) | $\Delta H^\ddagger (\tau)$<br>(kcal mol <sup>-1</sup> ) |
|-------------|---|---|---|
| NATA        | –   | 4.5   | –   |
| LADH        | 12.5  | 10.5  | 26.0  |
| Az          | 9.1   | 22.0  | 24.0  |
| AP          | 10.3  | 20.3  | 32.0  |
| Rnase T1    | –   | 5.5   | 9.6   |
| $\beta$ -LG | 10.0  | 8   | 7.0   |
| GAPDH       | 8.3   | 10  | 10.8  |

few Ångströms, the quenching reaction occurs efficiently through space and, in the case of RNase T1, the two rate constants may simply represent quenching from O<sub>2</sub> in the aqueous phase. As the separation increased, the through-space rate dropped dramatically, and O<sub>2</sub> migration through the protein became the dominant quenching pathway. Slow migration may have escaped detection with fluorescence quenching simply because at the large O<sub>2</sub> concentrations needed to affect these inaccessible residues one or more O<sub>2</sub> molecules were always inside the protein.

### 3.2. Temperature effects on quenching of $\beta$ -LG and GAPDH phosphorescence

The temperature dependence of  $kq_{O_2}$  in the range 0–50°C is shown in the Arrhenius plots of Fig. 4a. The slope of the best straight line through the data yielded activation enthalpies of 12.4 and 8.3 kcal/mol for  $\beta$ -LG and GAPDH, respectively (Table 2). These values of  $\Delta H^\ddagger$  were three times larger than for O<sub>2</sub> diffusion in water (3.1 kcal/mol), [6] but similar to those found for O<sub>2</sub> diffusion in polystyrene (7.1 kcal/mol), polycarbonate (9.5 kcal/mol) plastics [18], and to those measured previously for other proteins [8].

For these proteins, thermal activation parameters were also determined for acrylamide quenching and  $\tau_0$ , and the results are shown in Fig. 4b,c, respectively. Again, between 0 and 50°C, the plots were essentially linear and the values of activation enthalpies derived from their slopes (Table 2) were close to those obtained for the migration

of O<sub>2</sub>. This result indicated that for both proteins, in spite of the presumably different amplitudes of the motions involved in O<sub>2</sub> and acrylamide migration, the energy barriers of the underlying structural fluctuations were rather similar.  $\Delta H^\ddagger$  was also similar for  $\eta_{\tau_0}$ .

It is noteworthy that for all the proteins examined to date, the activation enthalpies for O<sub>2</sub> quenching were rather similar, ranging from 8.3 to 12.5 kcal/mol, in spite of the depth of the chromophore and the rigidity of its environment (Table 2). This result implied that the small amplitude fluctuations that permit the migration of O<sub>2</sub> are energetically similar throughout the protein matrix. In contrast, Fig. 5 shows that the  $\Delta H^\ddagger$  value derived for  $kq_{acr}$  and  $\eta_{\tau_0}$  were more strongly dependent on the fluidity of the structure about the Trp residues, becoming larger the higher the viscosity of the protein matrix. Similar conclusions have been drawn from the vast literature on hydrogen exchange studies [2,19,20]. These point out that the wide range of exchange rates: rapid for solvent accessible, flexible regions of the macromolecule, very slow for deeply buried amides, are also correlated with small ( $\sim 10$  kcal mol<sup>-1</sup>) and large ( $\sim 60$  kcal mol<sup>-1</sup>) activation energies, respectively. While the constancy of the activation enthalpy for the migration of O<sub>2</sub> was, at first, surprising, it has already been shown that oxygen diffuses in hydrocarbon polymers between 10 and 100 times more rapidly than predicted from the bulk viscosity [21] and, therefore, relatively free O<sub>2</sub> migration would be expected through proteins and biological membranes. *H-D*



exchange data point out that this is not a property of water molecules or its ions.

The results of the present study have shown that the magnitude of the phosphorescence quenching rate constant for oxygen was directly

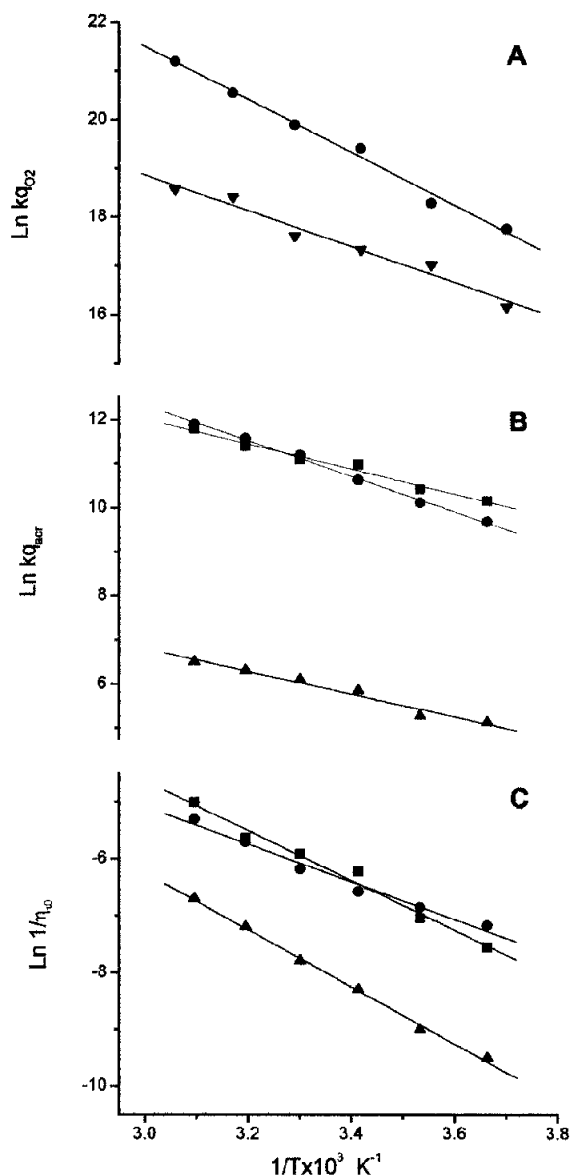


Fig. 4. Arrhenius plots of the  $O_2$  and acrylamide quenching rate constant [ $kq_{O_2}$  (a) and  $kq_{acr}$  (b)] and of  $1/\eta_{r0}$  (c), obtained over the 0–50°C temperature interval. The proteins samples are: (■) RNase T1, (●)  $\beta$ -LG and (▲) GAPDH.

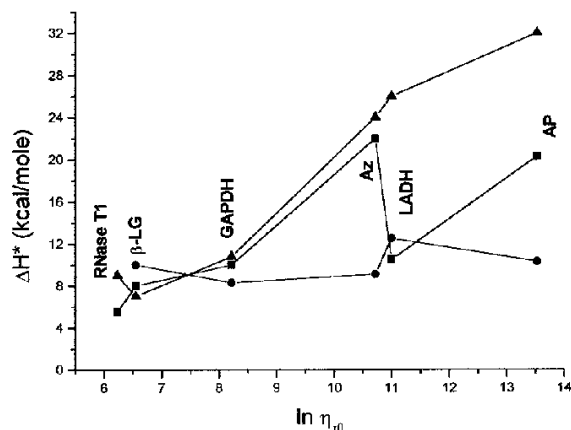


Fig. 5. Dependence of the activation enthalpies of  $1/\eta_{r0}$  (▲) and of the  $O_2$  (●) and acrylamide (■) quenching rate constants on the viscosity derived from  $\tau_0$  at 20°C for the proteins of Table 1.

correlated to the rigidity of the protein matrix surrounding the chromophore even for more peripheral and flexible regions. If the rate was dependent on the fluidity of the matrix, the small amplitude structural fluctuations that were involved were characterised by a similar activation energy throughout the protein structure.

## References

- [1] L.E. Kay, Protein dynamics from NMR, *Nature Struct. Biol.* 5 (S) (1998) 513–517.
- [2] K.T. Hitchens, R.G. Bryant, Pressure dependence of amide hydrogen–deuterium exchange rates for individual sites in T4 lysozyme, *Biochemistry* 37 (1998) 5878–5887.
- [3] M.R. Eftink, Topics in fluorescence spectroscopy, in: J.R. Lakowicz (Ed.), *Principles*, 2, Plenum Press, New York and London, 1991, pp. 53–126.
- [4] J.M. Vanderkooi, Topics in fluorescence spectroscopy, in: J.R. Lakowicz (Ed.), *Biochemical Applications*, 3, Plenum Press, New York and London, 1991, pp. 113–136.
- [5] P. Cioni, G.B. Strambini, Acrylamide quenching of protein phosphorescence as a monitor of structural fluctuations in the globular fold, *J. Am. Chem. Soc.* 120 (1998) 11749–11757.
- [6] J.R. Lakowicz, G. Weber, Quenching of protein fluorescence by oxygen. Detection of structural fluctuations in proteins on the nanosecond time scale, *Biochemistry* 12 (1973) 4171–4179.
- [7] P. Cioni, G.B. Strambini, Pressure–temperature effects on protein flexibility from acrylamide quenching of protein phosphorescence, *J. Mol. Biol.* 291 (1999) 955–964.

- [8] G.B. Strambini, P. Cioni, Pressure–temperature effects on oxygen quenching of protein phosphorescence, *J. Am. Chem. Soc.* 121 (1999) 8337–8344.
- [9] G.B. Strambini, M. Gonnelli, Tryptophan phosphorescence in fluid solution, *J. Am. Chem. Soc.* 117 (1995) 7646–7651.
- [10] M. Gonnelli, A. Puntoni, G.B. Strambini, Tryptophan phosphorescence of ribonuclease T1 as a probe of protein flexibility, *J. Fluorescence* 2 (1992) 157–165.
- [11] E. Gabellieri, G.B. Strambini, Phosphorescence properties of Trp-84 and Trp-310 in glyceraldehyde-3-phosphate dehydrogenase from *Bacillus stearothermophilus*, *Biophys. Chem.* 33 (1989) 257–264.
- [12] P. Busti, C.A. Gatti, N.J. Delorenzi, Some aspects of  $\beta$ -lactoglobulin structural properties in solution studied by fluorescence quenching, *Int. J. Biol. Macromol.* 23 (1998) 143–148.
- [13] V. Subramanian, D.G. Steel, A. Gafni, In vitro renaturation of bovine-lactoglobulin A leads to a biologically active but incompletely refolded state, *Protein Science* 5 (1996) 2089–2094.
- [14] G.B. Strambini, E. Gabellieri, Phosphorescence properties and protein structure surrounding tryptophan residues in yeast, pig and rabbit glyceraldehyde-3-phosphate-dehydrogenase, *Biochemistry* 28 (1989) 160–166.
- [15] M. Gonnelli, G.B. Strambini, Phosphorescence lifetime of tryptophan in proteins, *Biochemistry* 34 (1995) 13847–13857.
- [16] G.B. Strambini, Quenching of alkaline phosphatase phosphorescence by O<sub>2</sub> and NO. Evidence for inflexible regions of protein structure, *Biophys. J.* 52 (1987) 23–28.
- [17] D.V. Bent, E. Hayon, Excited state chemistry of aromatic amino acids and related peptides. III. Tryptophan, *J. Am. Chem. Soc.* 97 (1975) 2612–2619.
- [18] Y. Gao, A.M. Baca, B. Wang, P.R. Ogilby, Activation barriers for oxygen diffusion in polystyrene and polycarbonate glasses: effects of low molecular weight additives, *Macromolecules* 27 (1994) 7041–7048.
- [19] R. Li, C. Woodward, The hydrogen exchange core and protein folding, *Protein Sciences* 8 (1999) 1571–1591.
- [20] B.B. Kragelund, B. Heinemann, J. Knudsen, F.M. Poulsen, Mapping the lifetimes of local opening events in a native state protein, *Protein Sciences* 7 (1998) 2237–2248.
- [21] W.K. Subczynski, J.S. Hyde, Diffusion of oxygen in water and hydrocarbons using an electron spin resonance spin-label technique, *Biophys. J.* 45 (1984) 743–748.